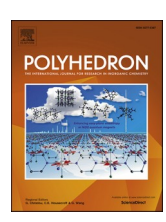


Contents lists available at ScienceDirect

Polyhedron

journal homepage: www.elsevier.com/locate/poly





Bis(*N*-xylyl-imino)phenyl "NCN" iridium pincer complexes. Thermodynamics of ligand binding and C—C bond cleavage[★]

Soumyadipa Das, Souvik Mandal, Santanu Malakar, Thomas J. Emge, Alan S. Goldman *

Department of Chemistry and Chemical Biology, Rutgers, The State University of New Jersey, New Brunswick, NJ 08854, United States

ARTICLE INFO

Keywords: C-C bond cleavage Metal-ligand bond strengths Iridium Pincer ligands Phenyldiimine

ABSTRACT

Iridium dibromide complexes of the phenyldiimine ligand 2,6-bis(1-((2,6-dimethylphenyl)imino)ethyl)phenyl, trans-(XyPhDI)IrBr₂L, have been synthesized, and relative Ir-L BDFEs have been experimentally determined for a wide range of corresponding adducts of ligands L. An estimate of the absolute enthalpy of Ir-L binding has been obtained from dynamic NMR measurements. The results of DFT calculations are in very good agreement with the relative and absolute experimental values. Computational studies were extended to the formation of adducts of (XyPhDI)IrH₂ and (XyPhDI)IrI, as well as other (pincer)IrI fragments, (Phebox)IrI and (PCP)IrI, to enable a comparison of electronic and steric effects with these archetypal pincer ligands. Attempts to reduce (XyPhDI) IrBr₂(MeCN) to a hydride or an IrI complex yielded a dinuclear CN-bridged complex with a methyl ligand on the cyanide-C-bound Ir center (characterized by scXRD), indicating that C-CN bond cleavage took place at that Ir center. DFT calculations indicate that the C-CN bond cleavage occurs at one Ir center with strong assistance by coordination of the CN nitrogen to the other Ir center.

1. Introduction

Iridium complexes bearing 2,6-bisphosphinomethyl aryl (PCP motif) and many related pincer ligands, including those with PNP, PPP, and bis (NHC)aryl (CCC) motifs, have been explored and developed extensively in the past 25 years. In particular such complexes have seen great success in C-H bond activation including catalytic alkane dehydrogenation and tandem reactions based upon dehydrogenation[1-11], as well as reactions involving cleavage and formation of C-O[12,13], N-H [14–16], and other strong bonds[17]. Iridium complexes of pincer ligands with terminal N-coordinating groups (e.g. NCN-type, such as 2,6bis-oxazolinephenyl, i.e. Phebox) have also seen development in catalysis and strong-bond activation. This chemistry, however, has typically not been analogous to that of the aforementioned ligands with phosphino- or carbene-coordinating "arms" (terminal groups) which largely operates via Ir(I) complexes. Instead, the chemistry of such NCN-iridium complexes has largely focused on Ir(III) carboxylate complexes that are believed to operate via concerted metalation-deprotonation (CMD) or other mechanisms involving high-oxidation complexes [18-25].

N-coordinating groups potentially offer significant advantages over P-coordinating and other "soft" groups, including ease of ligand

In this context we wished to explore the chemistry of an NCN complex with a relatively bulky N–coordinating group, and particularly one in which the steric bulk is not positioned only near the coordination site trans to the coordinating aryl carbon as in the case of Phebox. Toward this end we have synthesized adducts, 1-L, of the iridium dibromide complex of the phenyldiimine ligand, 2,6–bis(1–((2,6-dimethylphenyl) imino)ethyl)phenyl (XyPhDI). The complexes isolated represent somewhat unusual examples of late-metal pincer complexes bearing two electron-withdrawing low-field ancillary ligands (bromides). We have investigated the thermodynamics of the binding of the various ligands, L. DFT calculations are found to be in very good agreement with the experimental results. Encouraged by this agreement, we compare these

E-mail address: alan.goldman@rutgers.edu (A.S. Goldman).

synthesis, cost, and resistance to oxidation. From a fundamental perspective, it is of interest to understand the effect of such variations on catalytic or stoichiometric reactivity. However, whereas PXP-type pincer ligands (typically X=C or N) largely incorporate sterically demanding phosphino groups (e.g. P^tBu_2 or P^iPr_2), the NXN pincer ligands explored in this context have largely made use of groups such as oxazolines, which are much less bulky, and in which the limited steric bulk is positioned very differently than in the PCP complexes. These factors obfuscate any meaningful comparisons.

 $^{^{\}star}\,$ Dedicated to Prof. Peter T. Wolczanski on the occasion of his 70th birthday

^{*} Corresponding author.

results with binding thermodynamics calculated for the corresponding hydrides, and for the Ir(I) complexes of ^{Xy}PhDI and other pincer ligands. In an effort to synthesize the dihydride, which is of particular interest as a precursor of the corresponding Ir(I) fragment, we treated the dibromide precursor **1-MeCN** with KO^fBu under H₂ atmosphere. This resulted in the formation of a bimetallic species, the structure of which was determined crystallographically. Remarkably the molecular structure revealed that one equivalent CH₃CN had been hydrogenated to give ethylamine, and a second equivalent had undergone C—C bond cleavage to give an iridium center with a methyl and C-bound cyanide bridged to the second metal center.

2. Results and discussion

2.1. Synthesis of (XYPhDI)Ir complexes

Experimental results. 1,1'-(2-bromo-1,3-phenylene)bis(N-(2,6-dimethylphenyl)ethan-1-imine)[26] (XyPhDI-Br) was metalated by the reaction with [Ir(COD)Cl]₂ (COD = 1,5-cyclooctadiene) (Scheme 1) following the procedure reported by Oakley *et al.* for synthesis of aldimine analogues [27]. Crystals of 1–MeCN were grown by diffusion of pentane into a THF solution at room temperature, and the molecular structure was determined by scXRD (Fig. 1).

Acetonitrile was displaced from **1-MeCN** by reaction with 1.2 equiv of pyridine, PMe₃, N-ethylamine, or P(OMe)₃, or CO (1 atm), to give **1-py**, **1-PMe**₃, **1-NH**₂Et, **1-P(OMe)**₃ and **1-CO** respectively. Their molecular structures are shown in Fig. 2a-e.

Bubbling ethylene through a toluene solution of 1-MeCN to dryness yielded a solid that was redissolved in benzene under argon atmosphere. Crystals were obtained by slow evaporation and the molecular structure of the product, $1-C_2H_4$, was determined by scXRD (Fig. 2f).

Addition of ethylene atmosphere to a toluene solution of **1-MeCN** (without bubbling to dryness) led to a mixture of **1-MeCN** and **1-C₂H₄**. The equilibrium of Scheme 2 was established with $K_{eq}=0.181~(\Delta G^{\circ}=1.0~kcal/mol)$.

Bubbling solutions of $1\text{-}C_2H_4$ or 1-MeCN to dryness with N_2 gas resulted in no substitution, nor did the analogous approach lead to substitution with H_2 gas. It appears that these species bind much more weakly than C_2H_4 , or acetonitrile, if at all. Likewise addition of 1-hexene to a solution of $1\text{-}C_2H_4$ did not result in any observable substitution.

Addition of CO (1.9 atm) to a benzene- d_6 solution of **1-PMe**₃ did not result in any substitution or other reaction. Conversely, however, addition of 1.2 equiv PMe₃ to a solution of **1-CO** resulted in complete conversion to **1-PMe**₃. Given that CO typically binds very strongly to

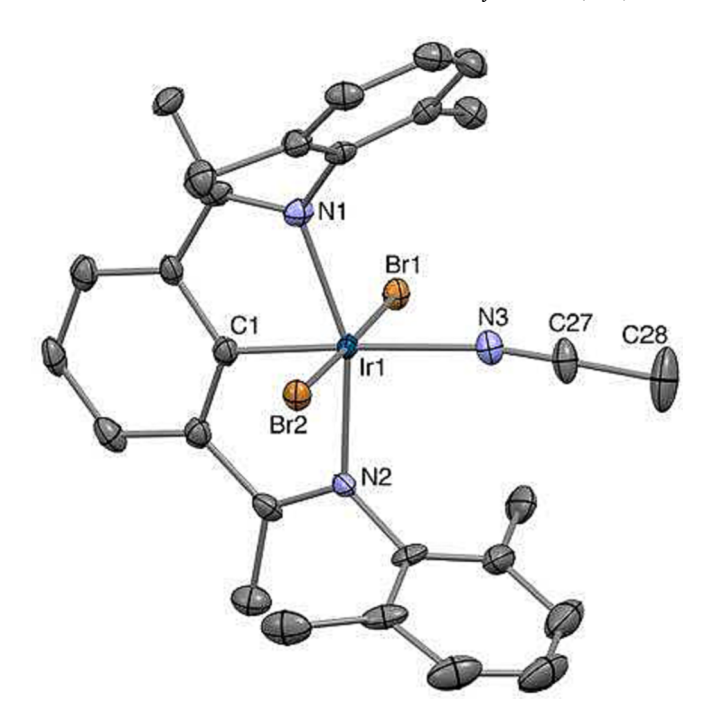


Fig. 1. Crystallographically determined molecular structure of 1-MeCN.

iridium complexes, including Ir(III) complexes, we found this result to be somewhat intriguing [28,29].

2.2. Thermodynamics of ligand binding

2.2.1. Relative energies of ligand binding to (Xy PhDI)Ir: Experimental and computational results

Equilibrium binding constants were determined for various pairs of ligands. In all cases the equilibrium was reached from both directions, by starting with a given complex 1-L, adding the complementary ligand L', waiting until equilibrium was apparently reached, and then adding an additional quantity of ligand L. K_{eq} ([ML'eq][Leq]/[MLeq][L'eq] for each ligand pair L/L') was determined for the following ligand pairs at 25 °C: MeCN/C2H4, $K_{eq}=0.181$ (Scheme 2); MeCN/ tBuNH_2 , $K_{eq}=32.0$; $^tBuNH_2/^iPrNH_2$, $K_{eq}=48.2$; $^tPrNH_2/py$, $K_{eq}=3.71$; py/EtNH2, $K_{eq}=2.63$; py/CO, $K_{eq}=13.8$; EtNH2/CO, $K_{eq}=4.95$; EtNH2/PPh2Me, $K_{eq}=2.15$. For PPh2Me/P(OMe)3, $K_{eq}=29.2$ was determined at 80 °C. The corresponding relative free energies of binding are given in Table 1.

Electronic structure (DFT) calculations were then conducted, initially for those complexes that were studied experimentally. Geometries were optimized in the gas phase using the M06 functional [30] and split valence basis set 6-31G(d,p) for C, H, N, O and P[31–35]. For Ir, the Stuttgart-Dresden effective core potential was used for the 60 core electrons; the associated basis set was used for the 17 valence electrons (SDD) [36]. All calculations were done at standard conditions of temperature (298.15 K) and pressure (1 atm); full details are given in the SI. Ir-L binding energies were calculated and are given in Table 2 (absolute

Scheme 1. Synthesis of 1-MeCN.

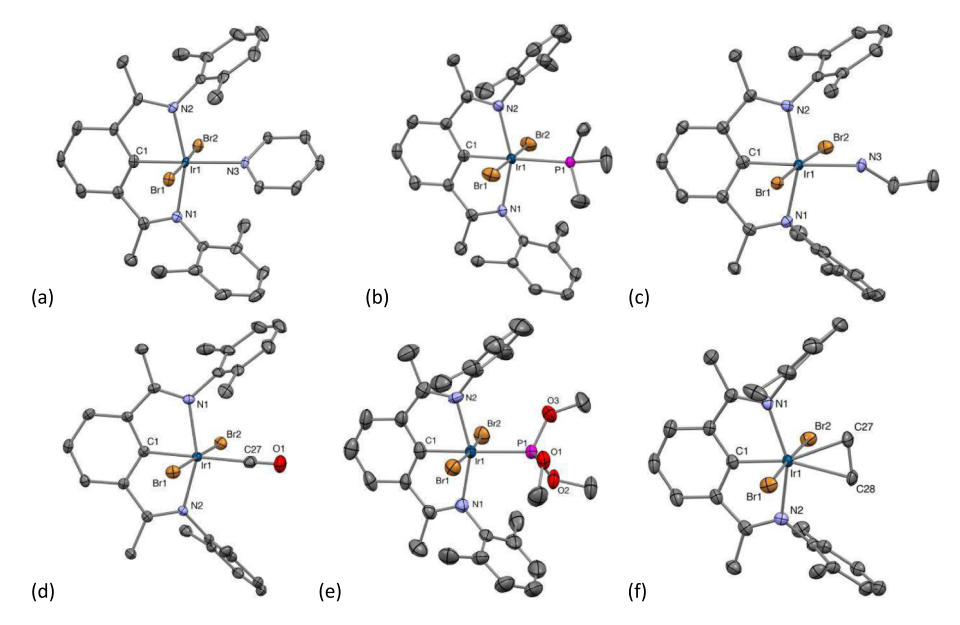


Fig. 2. Crystallographically determined molecular structures of (a) 1-py (b) 1-PMe₃ (c) 1-NH₂Et (d) 1-CO (e) 1-P(OMe)₃ (f) 1-C₂H₄.

$$K_{eq} = 0.18$$

$$G = 1.0 \text{ kcal/mol}$$

$$C_6D_6, \text{ r.t.}$$

$$K_{eq} = 0.18$$

$$G = 1.0 \text{ kcal/mol}$$

$$C_6D_6, \text{ r.t.}$$

$$C_6D_6, \text{ r.t.}$$

Scheme 2. Equilibrium between 1-MeCN and 1-C₂H₄.

Table 1
Free energies of binding to 1 relative to 1-C₂H₄.

	. 0	2	
Ligand	Experimental	Calculated	$\Delta(\text{Calc}-\text{Exptl})$
H ₂	>0	12.28	-
N_2	>0	7.57	-
1-hexene	>0	3.00	-
C_2H_4	[0.0]	[0.0]	[0.0]
MeCN	-1.01	-0.82	0.19
t-BuNH ₂	-3.05	-4.01	-0.96
i-PrNH ₂	-5.34	-7.19	-1.85
pyridine	-6.11	-6.75	-0.64
EtNH ₂	-6.68	-7.58	-0.90
PPh ₂ Me	-7.13	-8.69	-1.56
CO	-7.64	-8.52	-0.88
$P(OMe)_3$	-9.49	-12.11	-2.62
PMe ₃	$\ll -9.5$	-13.72	-

BDFEs)(see SI for electronic energy, enthalpy and entropy of binding). The calculated relative free energies of binding are in excellent agreement with experimentally obtained values (Table 1). For those ligands for which relative binding free energies were obtained experimentally, the root-mean-square deviation of all calculated relative values compared with all relative values extrapolated from the experimental measurements is 0.8 kcal/mol[37]; we consider this to be very satisfactory agreement.

With potential ligands H_2 , N_2 and 1-hexene we were unable to observe any displacement of C_2H_4 ; this is in agreement with their calculated low energies of binding. For H_2 and N_2 in particular, the

failure to observe substitution or loss of $1-C_2H_4$, even after bubbling solutions of $1-C_2H_4$ to dryness with the respective gas (and thereby providing a very strong entropic driving force for substitution) indicates that these molecules bind particularly weakly to 1 (if at all). The very unfavorable calculated free binding energies are consistent with this result. At the other extreme, none of the ligands used in this study were able to displace PMe₃ to any observable extent, in accord with its calculated very high relative free binding energy (13.7 kcal/mol greater than ethylene, Table 1).

Having established the ability of the computational method to reliably calculate relative energies of binding to 1, we used such calculation to study binding of the same ligands to related Ir fragments, specifically the corresponding dihydride (2), and the 14-electron Ir(I) fragment, (Xy PhDI)Ir (3; no ancillary ligands) (Fig. 3). We calculate that for amines and phosphines, the variability of the energy of binding to these three fragments was fairly small, with bond dissociation free energies (BDFEs) for each ligand found to be within a range spanning 6 kcal/mol. In contrast, the BDFE of CO increased strongly over the series 1 < 2 < 3 with the free energy of CO binding to Ir(I) fragment 3 (37.4 kcal/mol) being 19.3 kcal/mol greater ($\Delta G_1 - \Delta G_3$) than binding to Ir(III) fragment 1 (18.1 kcal/mol). Presumably this large variability reflects the degree of increasing π -donating ability among the various fragments, and commensurately increased metal–ligand π -backbonding.

Perhaps more surprising, in our view, was the magnitude of the variation calculated for binding of N_2 . N_2 generally binds much more weakly than CO and the complexes calculated in this study suggest no exception to that rule (e.g. the calculated free energy of N_2 binding to 1

Table 2 Calculated free energies (ΔG° , kcal/mol) of binding of various ligands to trans-(Xy PhDI)IrBr₂ (1), trans-(Xy PhDI)IrH₂ (2)^a, (Xy PhDI)Ir (3), (Phebox)Ir (4), (IP PCP)Ir (5) and (IB uPCP)Ir (6).

L	$(^{Xy}PhDI)IrBr_2$	(^{Xy} PhDI)IrH ₂ ^a	(^{Xy} PhDI)Ir	(Phebox)Ir	(^{iPr} PCP)Ir	(^{tBu} PCP)Ir
H ₂	2.7	-5.5	-6.7	-9.2	-13.8	-9.5
N_2	-2.0	-10.3	-16.1	-17.2	-20.1	-19.2
1-hexene	-6.6	-12.9	-20.1	-15.1	-21.4	-8.0
C_2H_4	-9.6	-14.0	-22.6	-16.4	-23.7	-16.7
MeCN	-10.4	-14.0	-18.0	-16.4	-18.4	-17.1
^t BuNH ₂	-13.6	-19.1	-18.6	-9.1	-12.8	-5.5
pyridine	-16.3	-18.1	-18.8	-16.4	-17.2	-14.7
ⁱ PrNH ₂	-16.8	-21.2	-21.3	-11.3	-16.3	-10.7
EtNH ₂	-17.1	-20.3	-20.4	-13.2	-15.8	-13.9
CO	-18.1	-32.5	-37.4	-43.0	-49.3	-48.1
PPh ₂ Me	-18.3	-25.6	-23.9	-20.2	-32.6	-14.6
P(OMe) ₃	-21.7	-32.2	-33.1	-31.5	-45.9	-35.0
PMe ₃	-23.3	-28.2	-27.4	-17.8	-29.4	-17.0

(a) See reference [38].

is only 2.0 kcal/mol). But although N_2 is also generally considered to be a much weaker π -acceptor than CO[39] the variation of N_2 binding energies among the complexes is nearly as great as that found for CO; N_2 is calculated to bind 14.1 kcal/more strongly to fragment 3 than to fragment 1 ($\Delta G_1 - \Delta G_3$). NBO analysis of the CO and N_2 adducts of 1, 2 and 3 indicates, as expected, that CO is a better π -acceptor than N_2 (see SI). However, as the electron-donating ability of the fragment increases (1 < 2 < 3), the electronic occupancy of the ligand π * orbitals is calculated to increase approximately as much (actually slightly *more*) for N_2 than for CO [40]. This seems very consistent with the calculated increase in the Ir- N_2 BDE being comparable to the increase calculated for the Ir-CO BDE for this series of complexes.

Ethylene and 1-hexene show sensitivity to the nature of the fragment that is approximately equal to that of N_2 ($\Delta G_1 - \Delta G_3 = 13.0$ kcal/mol and 13.5 kcal/mol respectively) while trimethyl phosphite is comparably sensitive ($\Delta G_1 - \Delta G_3 = 11.4$ kcal/mol). Acetonitrile ($\Delta G_1 - \Delta G_3 = 7.6$ kcal/mol) shows variability somewhere in between that of the amine ligands and those ligands that are apparently very sensitive to π -donating ability (e.g. CO, N_2 , olefins).

 H_2 is calculated to add to the three (Xy PhDI)Ir fragments investigated to give a dihydrogen complex with a relatively short H—H distance varying only from 0.81 Å (1 - 1 - 1) to 0.85 Å (3 - 1 - 1). Thermodynamically, the binding energy shows moderate sensitivity to the nature of the iridium fragment (1 - 1

Generally speaking, our calculations predict that π -acceptor ligands such as CO, but also N2 and alkenes, bind much more strongly to the (Xy PhDI)Ir species with greater π -electron-donating ability ((Xy PhDI) IrH₂ and (Xy PhDI)Ir), with a sensitivity to π -electron-donating ability that is much greater than calculated for ligands such as amines; this is consistent with the most fundamental organometallic precepts and classical organometallic bonding descriptions. In such descriptions, CO is presented as a strong π -acceptor while amines are pure sigma donors or are even considered to be $\pi\text{-donors}$ as well as $\sigma\text{-donors}.$ From that perspective, however, it is noteworthy that the binding energy of Nethylamine for example is even slightly greater toward the more electron-rich iridium fragments; the model of simple donation seems inconsistent with these data. Moreover, the variation found for phosphines is very nearly equal to that for amines; this seems inconsistent with the former being considered even modest π -acceptors [41,42]. A full analysis of the origin of these effects is beyond the scope of this paper, but we plan to address these questions in future work.

2.2.2. Ligand binding to other (pincer)Ir(I) fragments

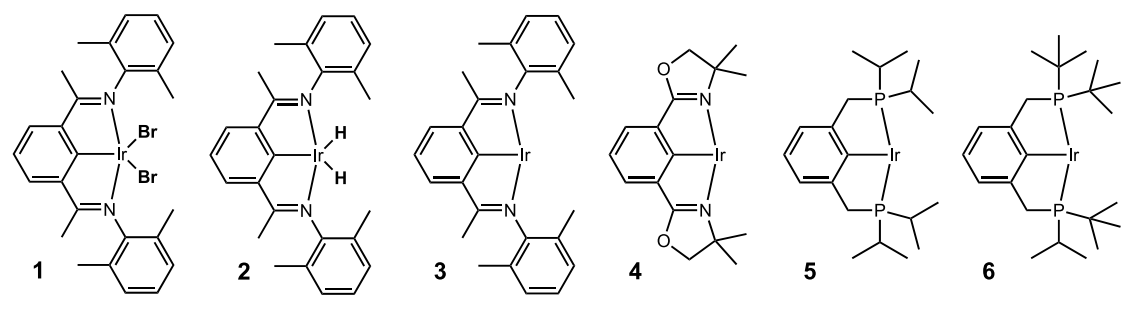
We have also calculated, for comparison with (^{Xy}PhDI)Ir, the energies of binding of monodentate ligands to the (pincer)Ir(I) fragments (Phebox)Ir, (^{iPr}PCP)Ir, and (^{tBu}PCP)Ir (Table 2 and Fig. 3). Of these, the Phebox pincer ligand is of course the most closely related of these to ^{Xy}PhDI, having the same diaminoaryl NCN motif. van Koten and co-

workers have shown that nickel complexes of these two pincer ligands have fairly similar redox properties as might be expected [26].

The sterically undemanding ligands H2, N2, and CO bind more strongly to the (Phebox)Ir fragment than to (XyPhDI)Ir, while acetonitrile binds slightly less strongly. This could suggest that (Phebox)Ir is a more π -electron-donating fragment but a slightly poorer σ -acceptor. Larger differences between Ir-L BDFEs of (Phebox)IrL versus (XyPhDI)IrL are seen in the case of larger ligands, with the binding to (Phebox)Ir being weaker in all cases. The respective complexes are four-coordinate d⁸, therefore approximately square planar, and therefore this indicates specifically that the binding site trans to the Ir-bound aryl carbon is more crowded in (Phebox)Ir than in (XyPhDI)Ir. Inspection of the calculated structures of the ^{Xy}PhDI complexes supports this conclusion. The *N*-xylyl groups are oriented so that this trans coordination site of the ^{Xy}PhDI complexes is significantly more open than that of (Phebox)Ir. For example, in the respective PMe3 complexes there are numerous close contacts ($d_{H-H} < 2.4 \text{ Å}$) between the Phebox methyl groups and the PMe₃ ligand (Fig. 4a), but no close contacts between coordinated PMe3 and the ^{Xy}PhDI ligand (Fig. 4b).

Notably, although the trans site of the (XyPhDI)Ir fragment is much more open than that of (Phebox)Ir, the sites cis to the Ir-bound carbon are fairly crowded in the case of (XyPhDI)Ir while extremely open in the case of (Phebox)Ir. This is illustrated in Fig. 5 with space filling models of the respective (pincer)Ir(PMe3) complexes and the Buried Volume maps of the (pincer)Ir fragments of Fig. 6 [43,44]. Qualitatively at least, the distribution of steric bulk in the (XyPhDI)Ir fragment resembles that of the (PCP)Ir fragments more closely than that of (Phebox)Ir, in that the (PCP)Ir fragments are also more crowded at the coordination sites cis to the Ir-bound carbon than at the trans sites. The symmetry of the (tBuPCP) Ir fragment (Fig. 6c) makes the qualitative resemblance to (XyPhDI)Ir (Fig. 6a) more apparent than for the (iPrPCP)Ir (Fig. 6d) fragment because the two i-propyl groups on each P atom are generally oriented in opposite directions (one tertiary C—H bond toward the Ir center and the other pointed away). Quantitatively however the Buried Volume calculations indicate that the (Xy PhDI)Ir fragment (W VBUR = 68.2 %) is much more similar to (^{iPr}PCP)Ir (67.3 %) than to (^{tBu}PCP)Ir (78.4 %).

To assess the magnitude of the effect of steric crowding at the coordination sites cis to the Ir-bound carbon in the (Xy PhDI)Ir unit, we calculated the thermodynamics of the (hypothetical) reaction of (Ar PhDI)Ir(CO) with Br₂ to give *trans*-(Ar PhDI)IrBr₂(CO), where Ar = xylyl (the present system) and Ar = phenyl (i.e. a model PhDI ligand lacking the xylyl methyl groups) (Fig. 7a). The addition of Br₂ is found to be 16 kcal/mol less favorable for the more crowded Xy PhDI complex. This effect is presumably entirely due to steric crowding, since any electronic effect is expected to be very small and to *favor* oxidative addition to the Xy PhDI complex. We also calculate that *trans*-addition of Br₂ to (phebox)Ir(CO) has a free energy approximately equal to that for (Ar PhDI)Ir(CO), 71.2 kcal/mol, consistent with these complexes both



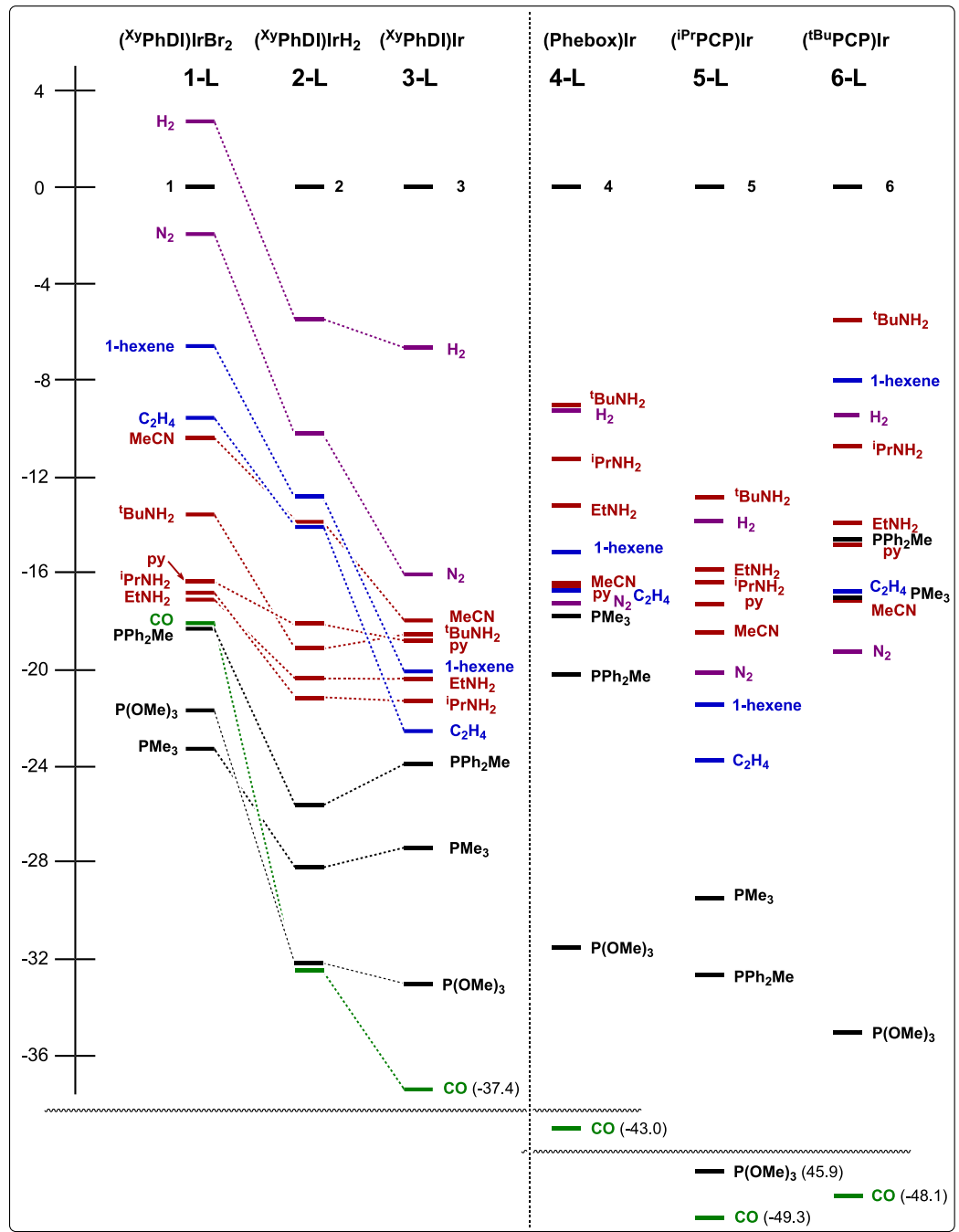


Fig. 3. Calculated free energies of binding of various ligands to fragments $\mathbf{1}-\mathbf{6}.$

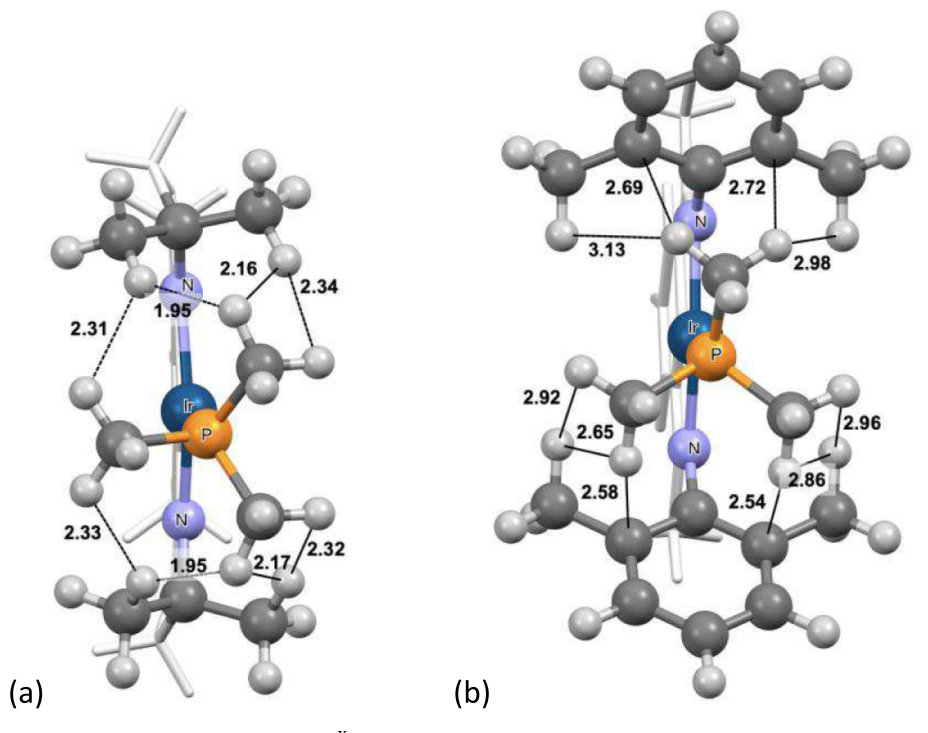


Fig. 4. DFT-calculated structures of (a) (Phebox)Ir(PMe₃) and (b) (^{Xy}PhDI)Ir(PMe₃) with closest contacts between PMe₃ and pincer ligand indicated (Å) (illustrating much more severe crowding in the Phebox complex).

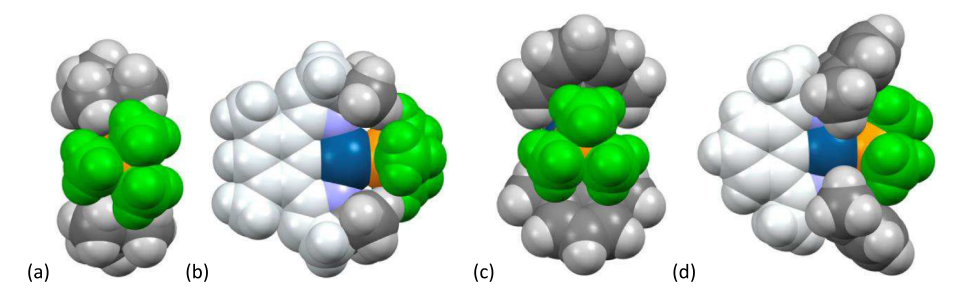


Fig. 5. DFT-calculated structures (space-filling models at 100% van der Waals radii) of (Phebox)Ir(PMe₃) (a and b) and (^{Xy}PhDI)Ir(PMe₃) (c and d). Viewed down Ir-C axis (a and c) and axis perpendicular to the plane of the pincer backbone (b and d) to illustrate the greater crowding of (Phebox)Ir at the site trans to the Ir-bond C atom, in contrast with the greater steric hindrance of (^{Xy}PhDI)Ir(PMe₃) at the sites cis to the Ir-bond C atom. PMe₃ methyl groups in green and non-coordinating atoms of the pincer backbones in light grey.

having negligible steric crowding at the cis coordination sites as would be expected (see Fig. 5).

The crowding at the cis positions of $trans-(^{Xy}PhDI)IrBr_2(CO)$ is clearly manifest in its geometric structure (Fig. 7b). The coordination sphere is distorted and the xylyl ring is canted so that one bromide ligand sits between the xylyl methyl groups and the CO ligand, while the other bromide is positioned between the methyl groups and the PhDI backbone. The corresponding C_{ipso} -Ir-Br angles are 94.4° and 82.3° respectively, as compared with the much more symmetrical coordination sphere of the truncated $trans-(^{Ph}PhDI)IrBr_2(CO)$, which has C_{ipso} -Ir-Br angles of 88.8° and 88.3°.

All ligands that we have studied are calculated to bind much more strongly to (^{iPr}PCP)Ir than to (Phebox)Ir (Fig. 3). Compared with ($^{Xy}PhDI$)Ir, however, the amines bind less strongly to (^{iPr}PCP)Ir while the phosphines bind more strongly to (^{iPr}PCP)Ir. The small π -accepting ligands bind more strongly to (^{iPr}PCP)Ir than to ($^{Xy}PhDI$)Ir, with CO in particular binding 12 kcal/more strongly, while P(OMe)₃ also binds much more strongly to (^{iPr}PCP)Ir (by 12.8 kcal/mol). P(OMe)₃ is known to be a good π -acceptor, but presumably much less π -accepting than CO. The greater energy of binding of P(OMe)₃ to (^{iPr}PCP)Ir versus ($^{Xy}PhDI$)Ir

may therefore be a combination of greater π -donating ability of the (iPr PCP)Ir fragment combined with a greater tendency to bind to the P-donating ligands generally, perhaps related to the "softness" of these ligands in contrast with the "hard" N-donors.

2.2.3. Kinetics of exchange with ethylene: Thermodynamic implications

At room temperature, the 1 HNMR spectrum of $1\text{-}C_2H_4$ in the presence of free C_2H_4 indicates rapid exchange of free and bound ethylene. Decoalescence of the respective 1 H NMR signals was observed at slightly reduced temperature, and the individual signals, attributable to free and bound C_2H_4 respectively, were sharp at 255 K. Dynamic NMR allowed determination of the rate constants for exchange, over the temperature range 255 K – 298 K (Table 3), by simulation using the dNMR feature in the program Topspin [45]. An Eyring plot (Fig. 8) of the rates thus obtained yielded activation parameters $\Delta H^{\ddagger} = 25.0$ kcal/mol and $\Delta S^{\ddagger} = 36.0 \pm 1.0$ cal/moledeg. The positive activation entropy indicates that the reaction proceeds via dissociation of ethylene, as would be expected of an 18-electron ethylene complex. The activation enthalpy is very close to the calculated *thermodynamic* value of the enthalpy of dissociation, $\Delta H^{\circ} = 23.7$ kcal/mol. Taken at face value, this would

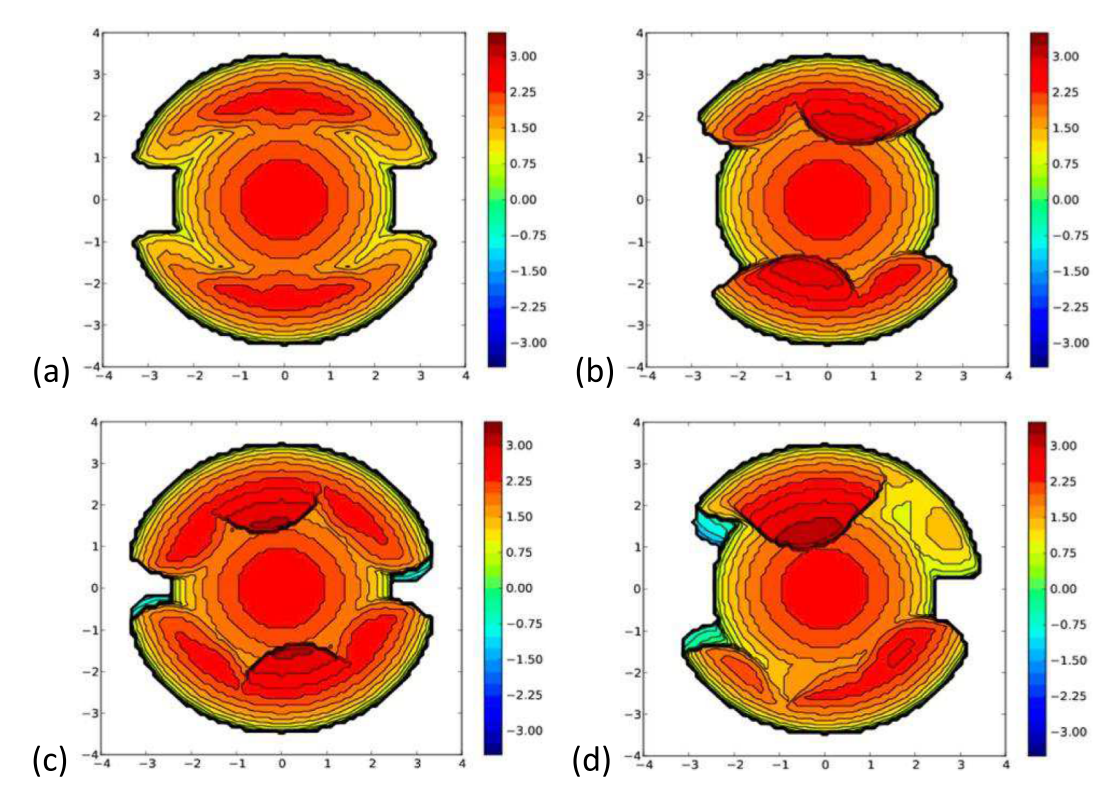


Fig. 6. Topographical ligand steric maps and percent Buried Volume (% V_{BUR}) [43,44] of (a) (Xy PhDI)Ir (68.2%) (b) (Phebox)Ir (64.0%) (c) (IBu PCP)Ir (78.4%) (d) (IP PCP)Ir (67.3%).

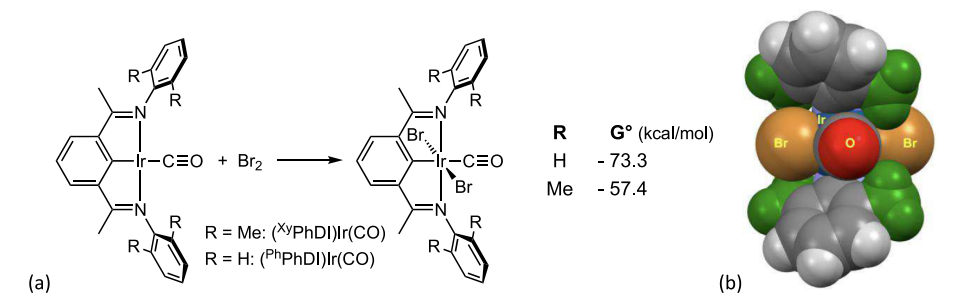


Fig. 7. (a) Oxidative addition of Br₂ to (ArPhDI)Ir(CO) to yield *trans*-(ArPhDI)IrBr₂(CO) and calculated free energies, indicating the magnitude of the thermodynamic effect of crowding at the positions cis to the Ir-bound carbon of the ArDI backbones. (b) Spacefilling model (at 100 % van der Waals radii)) of *trans*-(XyPhDI)IrBr₂(CO) (benzylic groups in green) highlighting the steric crowding and resulting distortion from idealized symmetry (C_{2v}).

 $\begin{tabular}{ll} \textbf{Table 3} \\ \textbf{Rates and free energy for exchange between free and 1-bound C_2H_4 obtained by dynamic NMR and simulations.} \end{tabular}$

T (K)	k (s ⁻¹)	ΔG [‡] (kcal/mol)		
298	190	14.3		
285	29.6	14.7		
275	5.66	15.1		
265	0.877	15.5		
255	0.138	15.9		

imply, as might also be expected, that addition of ethylene to the 16-electron dissociation product, 1, has a near-zero enthalpic barrier of approximately $\Delta H^{\ddagger}=1.3$ kcal/mol. These results offer experimental support for the DFT-calculated thermodynamic values for ethylene (albeit approximate). Accordingly, they also support the validity of the absolute values of the DFT-calculated binding free energies of those ligands for which the *relative* (to ethylene) binding free energies are in agreement with experimental values.

2.3. Cleavage of the C-C bond of acetonitrile

In an attempt to reduce **1-MeCN** to the corresponding dihydride or Ir (I) complex, the complex was treated with KO^IBu (3 equiv) in benzene under H_2 atmosphere and was left to stir at room temperature overnight under the hydrogen atmosphere. Benzene was evaporated and the solution was extracted with pentane to remove excess base. Crystals were grown under inert atmosphere at room temperature by diffusion of pentane into a concentrated benzene solution. Unexpectedly, scXRD revealed the product to be a binuclear bridging cyanide complex with the molecular structure as shown in Fig. 9. Although hydrides were not located unambiguously by crystallography, the ¹H NMR spectrum of the crystals, after dissolving in benzene- d_6 , indicated the presence of two equivalent hydride ligands (-26.5 ppm) in accord with formulation as $[(^{Xy}PhDI)Ir(Me)(H_2NEt)](\mu -CN)[(^{Xy}PhDI)IrH_2]$ (7).

The net reaction to give 7 thus involves hydrogenation of one molecule of $CH_3CN[46,47]$ (per molecule of binuclear product) and cleavage of the C—C bond of a second molecule of $CH_3CN[48]$. C—C bond cleavage generally, and cleavage of alkyl cyanides in particular, is

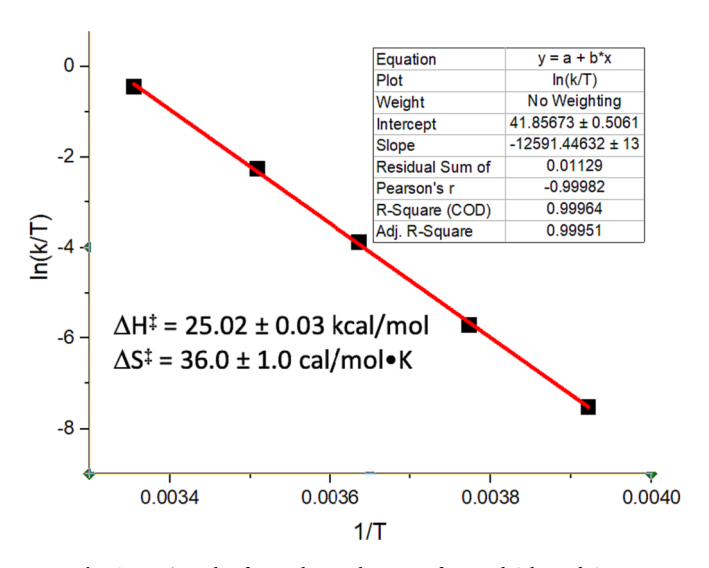


Fig. 8. Eyring plot for exchange between free and 1-bound C₂H_{4.}

a reaction of much interest [49–56]. The examples that are perhaps most closely related to the present work have been reported by Garcia and Jones [57–62].

We investigated the reaction of the (XyPhDI)Ir fragment with CH₃CN computationally and located a transition state for direct oxidative addition of the acetonitrile C-C bond. However the barrier of this reaction was calculated to be too high, at 33.1 kcal/mol, to account for the formation of 7 at room temperature. Lewis acids, however, have been reported to accelerate C-CN bond cleavage [58,63] or the reverse, C-CN reductive elimination[64,65]. (Notably, Garcia and Jones have reported an example where Lewis acid binding actually inhibited C-C cleavage [57]). Therefore, given that the nitrile group of 7 is bridging, we considered that the second (XyPhDI)Ir unit played a role in promoting the C-C cleavage reaction. In accord with this hypothesis, the free energy barrier to C—C cleavage was calculated to be only 10.4 kcal/mol when the acetonitrile N atom was coordinated to a (MePhDI)IrH2 fragment (the N-coordinated (PhDI)Ir moiety was truncated in the transition state, with xylyl groups replaced by methyl groups for computational simplicity; 3*-H₂; Fig. 10). Although the free energy of this binding is positive, $\Delta G^{\circ} = 7.7$ kcal/mol, due to a large unfavorable entropy term $(T\Delta S = -16.7 \text{ kcal/mol at } 298 \text{ K})$, the overall calculated barrier of C—C cleavage, $\Delta G^{\ddagger}=18.1$ kcal/mol, is still dramatically lowered by assistance from the second (PhDI)Ir center. The initial C—C cleavage product and the final, ethylamine-coordinated, product were calculated to be

significantly exergonic relative to 3-MeCN, 3-H₂, and EtNH₂.

The calculations indicate, remarkably, that in the transition states for C-CN cleavage, both metal assisted and non-assisted, the Ir–CN bond is significantly shorter in the transition states (1.94 Å and 1.96 Å for Irbridged and non-bridged respectively) than in the products in which the Ir-CN bond is fully formed (2.10 Å and 2.07 Å) (Fig. 11). Note, however, that as would generally be expected for an oxidative addition reaction, the Ir-CH₃ distance is significantly shorter in the products than in the transition states. Acetonitrile C—C oxidative addition by (dippe) Ni(0)[59] and Cp*(PMe₃)Rh(I)[60] (not assisted by a second metal) has been investigated computationally in detail by Jones. While our results are generally in agreement with those, in the Rh(I) case the M—CN bond in the TS (2.00 Å) was slightly longer[60] than in the C—C cleavage product (1.97 Å). In the case of Ni(0), however, as in the present systems the M—C bond was shorter in the TS (1.82 Å) than in the product (1.88 Å) although the difference was not as pronounced.

Alkyl cyanide elimination/C—C bond formation has been compared with alkyl migration to CO (i.e. CO insertion into M-alkyl bonds [65–67]. This perspective might help to rationalize this unusual example of a TS for C—C cleavage with a M-C distance shorter than that of the product with the fully formed M-C bond. For example, we have computationally studied alkyl migration to CO of Mn(CO)₅(CH₂Ar), and found that the M-CO bond in the migration transition state is shorter (1.82 Å) than in the carbonyl reactant (1.86 Å) or in the acyl product of migration (1.88 Å) [68]. Note also that in the transition states calculated in this work, as well as in the systems studied by Jones [59,60], there is a significant agostic interaction with the acetonitrile methyl C-H bond. In our studies of alkyl migration to CO (or alkyl migration from acyl ligand to metal) it was shown that formation of an analogous agostic interaction played a significant role in the energy of the transition state [68]; these shared feature would seem to further support the proposed relationship between alkyl migration and alkyl-CN cleavage/ elimination.

3. Conclusions

Iridium dibromide complexes of the phenyldiimine ligand 2,6-bis(1-((2,6-dimethylphenyl)imino)ethyl)phenyl have been synthesized, and the relative Ir-L BDFEs have been experimentally determined for a wide range of corresponding adducts of ligands L. An estimate of the absolute enthalpy of Ir-L binding has been obtained from dynamic NMR measurements. The results of DFT calculations are in very good agreement with the relative and absolute experimental values.

A computational study has been conducted, first comparing (^{Xy}PhDI) Br₂Ir-L BDFEs with Ir-L BDFEs of adducts *trans*-(^{Xy}PhDI)H₂IrL and

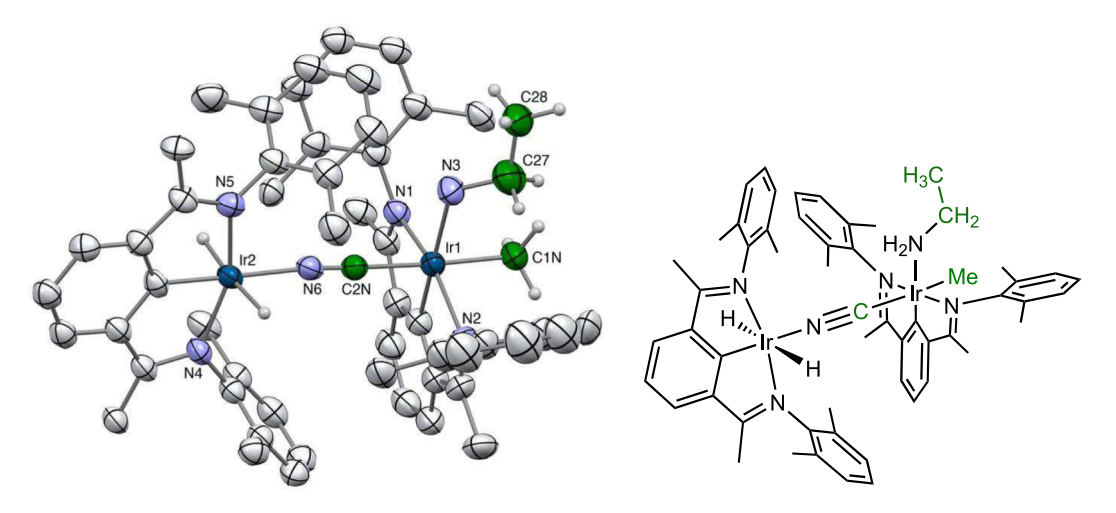


Fig. 9. Molecular structure of 7. H atoms except hydrides and those of the methyl and ethylamine ligands omitted for clarity. Carbon atoms of methyl and ethylamine ligands and bridging cyanide shown in green for emphasis.

Fig. 10. Calculated energy profile (free energies in kcal/mol) for oxidative addition of the C—C bond of acetonitrile by 1, assisted by (truncated) $1*-H_2$ and unassisted. Untruncated initial and final products also shown. (Selected distances in Å).

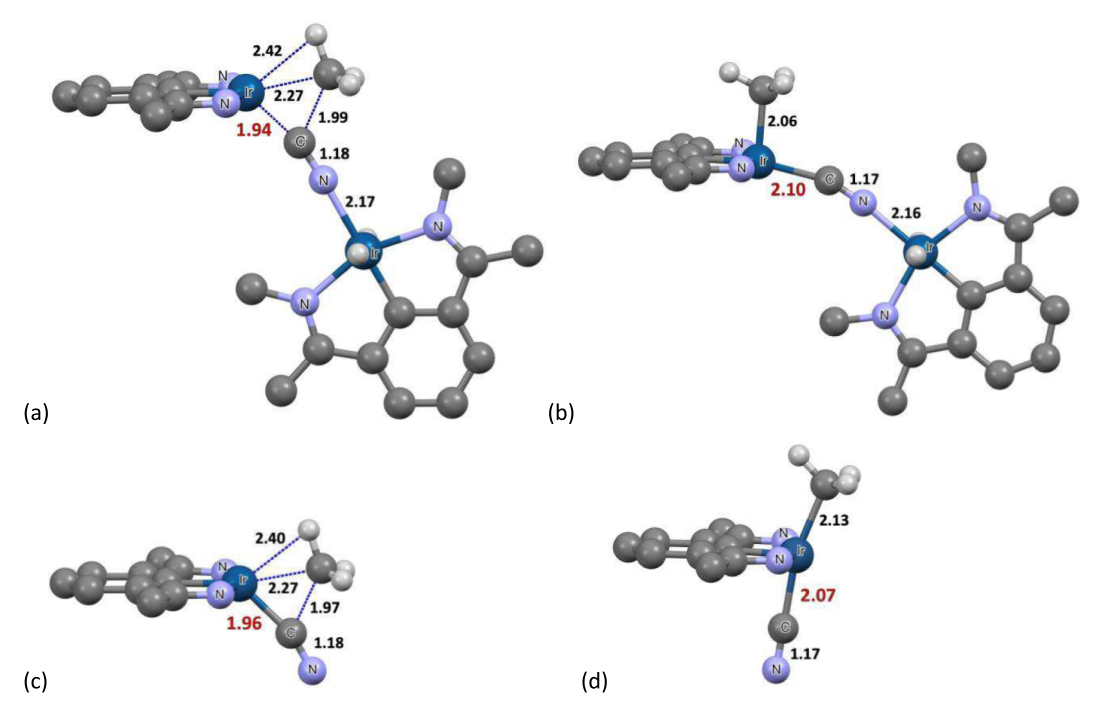


Fig. 11. Calculated transition state (a) and product (b) of oxidative addition of the C—C bond of acetonitrile by **3**, assisted by **3*–H₂**. Transition state (c) and product (d) of "unassisted" C-CN addition by **3**. *N*-mesityl groups of **3**, and most H atoms, omitted for clarity.

(Xy PhDI)IrL. The Ir-L BDFEs are all greater for the dihydride than for the dibromide, with the difference being much more pronounced for π -accepting ligands. BDFEs of π -accepting ligands are even markedly greater still for the Ir(I) complexes (Xy PhDI)IrL versus trans-(Xy PhDI) $_{1}$ IrL, while there is little difference for ligands that are less π -accepting.

We also compared (Xy PhDI)Ir-L BDFEs with BDFEs of (pincer)Ir-L complexes for pincers Phebox, iPr PCP, and tBu PCP. The (Phebox)Ir fragment, compared with (Xy PhDI)Ir, forms slightly stronger bonds with the smallest π –accepting ligands, but (Phebox)Ir-L bonds are significantly weaker with bulky ligands, particularly those that are not significantly π -accepting. Although Buried Volume calculations indicate

that the (Phebox)Ir fragment has overall greater "unburied" volume than (Xy PhDI)Ir, the coordination site occupied by L in the four-coordinate d⁸ (pincer)IrL complexes (i.e. the site trans to Ir-bound aryl C) is significantly more crowded in (Phebox)Ir. The motif of (Xy PhDI)Ir, with greater steric crowding at the cis sites and a more open site trans to the aryl C is also found for both (IP PCP)Ir and (IBu PCP)Ir pincer ligands. The (R PCP)Ir fragments appear to be more π -donating than the Phebox or PhDI fragments, as illustrated by stronger binding to CO or N₂, but with respect to sterically demanding ligands, the BDFEs of (Xy PhDI)IrL are somewhere between those of the very crowded (IBu PCP)Ir and the much less crowded (IP PCP)Ir.

An attempt to convert (Xy PhDI)IrBr₂(MeCN) to a hydride or possibly an Ir(I) complex yielded an unexpected dinuclear cyano-bridged complex with *N*-ethylamine (presumably the product of hydrogenation of one mol acetonitrile) coordinated to one metal center, and a methyl ligand on the cyanide carbon-bound iridium center, indicating the occurrence of C-CN bond cleavage at the latter Ir center. DFT calculations indicate that the C-CN bond cleavage occurs at one Ir center with strong assistance by coordination of the CN nitrogen to the other center. At the metal center effecting the C-CN addition the transition state is calculated to strongly resemble a transition state for alkyl migration to CO or the microscopic reverse, C—C bond cleavage of an acyl ligand. Similarities include a M—CX (X=N or O) bond distance in the TS that is shorter than that in the M—CX C—C cleavage product, and a strong agostic interaction with a C—H bond of the alkyl group being cleaved from CX.

The inference of C—C cleavage by the (^{Xy}PhDI)Ir(I) fragment may suggest promising activity, related but distinct from the chemistry of (^RPCP)Ir(I) fragments, if such a species can be generated in the absence of acetonitrile.

CRediT authorship contribution statement

Soumyadipa Das: Conceptualization, Data curation, Formal analysis, Investigation, Writing – original draft, Writing – review & editing. **Souvik Mandal:** Conceptualization, Formal analysis, Investigation, Writing – review & editing. **Santanu Malakar:** . **Thomas J. Emge:** Investigation, Formal analysis, Writing – review & editing. **Alan S. Goldman:** Investigation, Formal analysis, Writing – review & editing, Conceptualization, Supervision, Writing – original draft.

Declaration of competing interest

The authors declare that they have no known competing financial interests or personal relationships that could have appeared to influence the work reported in this paper.

Data availability

Data will be made available on request.

Acknowledgments

This work was supported by the U. S. Department of Energy Office of Science (DE-SC0020139). The National Science Foundation is acknowledged for grant CHE-2117792 for acquisition of the X-ray diffractometer used to obtain all scXRD structures for this work.

Appendix A. Supplementary data

Supplementary data to this article can be found online at https://doi. org/10.1016/j.poly.2024.116853.

References

- [1] Y. Wang, Z. Huang, G. Liu, Z. Huang, A New Paradigm in Pincer Iridium Chemistry: PCN Complexes for (De)Hydrogenation Catalysis and Beyond, Acc. Chem. Res. 55 (2022) 2148–2161, https://doi.org/10.1021/acs.accounts.2c00311.
- [2] B.M. Gordon, N. Lease, T.J. Emge, F. Hasanayn, A.S. Goldman, Reactivity of Iridium Complexes of a Triphosphorus-Pincer Ligand Based on a Secondary Phosphine. Catalytic Alkane Dehydrogenation and the Origin of Extremely High Activity, J. Am. Chem. Soc. 144 (9) (2022) 4133–4146, https://doi.org/10.1021/ iosg.1c1.3200
- [3] A.D.R. Shada, A.J.M. Miller, T.J. Emge, A.S. Goldman, Catalytic Dehydrogenation of Alkanes by PCP-Pincer Iridium Complexes Using Proton and Electron Acceptors, ACS Catal. 11 (2021) 3009–3016, https://doi.org/10.1021/acscatal.0c05160.
- [4] K. Das, A. Kumar, Alkane dehydrogenation reactions catalyzed by pincer-metal complexes, Adv. Organomet. Chem. 72 (2019) 1–57, https://doi.org/10.1016/bs. adomc.2019.02.0041.

- [5] X. Tang, X. Jia, Z. Huang, Thermal, Catalytic Conversion of Alkanes to Linear Aldehydes and Linear Amines, J. Am. Chem. Soc. 140 (11) (2018) 4157–4163, https://doi.org/10.1021/jacs.8b01526.
- [6] A. Kumar, T.M. Bhatti, A.S. Goldman, Dehydrogenation of Alkanes and Aliphatic Groups by Pincer-Ligated Metal Complexes, Chem. Rev. 117 (19) (2017) 12357–12384, https://doi.org/10.1021/acs.chemrev.7b00247.
- [7] X. Jia, Z. Huang, Conversion of alkanes to linear alkylsilanes using an iridium-iron-catalyzed tandem dehydrogenation-isomerization-hydrosilylation, Nat. Chem. 8
 (2) (2016) 157–161, https://doi.org/10.1038/nchem.2417.
- [8] W. Yao, X. Jia, X. Leng, A.S. Goldman, M. Brookhart, Z. Huang, Catalytic Alkane Transfer-Dehydrogenation by PSCOP Iridium Pincer Complexes, Polyhedron 116 (2016) 12–19, https://doi.org/10.1016/j.poly.2016.02.044.
- M.C. Haibach, S. Kundu, M. Brookhart, A.S. Goldman, Alkane Metathesis by Tandem Alkane-Dehydrogenation-Olefin-Metathesis Catalysis and Related Chemistry, Acc. Chem. Res. 45 (2012) 947–958, https://doi.org/10.1021/ ar3000713
- [10] J. Choi, A.S. Goldman, Ir-Catalyzed Functionalization of C–H Bonds, Top. Organomet. Chem. 34 (2011) 139–167, https://doi.org/10.1007/978-3-642-15334-1
- [11] A. Ray, K. Zhu, Y.V. Kissin, A.E. Cherian, G.W. Coates, A.S. Goldman, Dehydrogenation of aliphatic polyolefins catalyzed by pincer-ligated iridium complexes, Chem. Commun. (2005) 3388–3390, https://doi.org/10.1039/ B502120K.
- [12] J. Choi, Y. Choliy, X. Zhang, T.J. Emge, K. Krogh-Jespersen, A.S. Goldman, Cleavage of sp³ C-O Bonds via Oxidative Addition of C-H Bonds, J. Am. Chem. Soc. 131 (43) (2009) 15627–15629, https://doi.org/10.1021/ja906930u.
- [13] M.C. Haibach, C. Guan, D.Y. Wang, B. Li, N. Lease, A.M. Steffens, K. Krogh-Jespersen, A.S. Goldman, Olefin Hydroaryloxylation Catalyzed by Pincer-Iridium Complexes, J. Am. Chem. Soc. 135 (40) (2013) 15062–15070, https://doi.org/10.1021/ja404566v.
- [14] M. Kanzelberger, X. Zhang, T.J. Emge, A.S. Goldman, J. Zhao, C. Incarvito, J. F. Hartwig, Distinct Thermodynamics for the Formation and Cleavage of N-H Bonds in Aniline and Ammonia. Directly-Observed Reductive Elimination of Ammonia from an Isolated Amido Hydride Complex, J. Am. Chem. Soc. 125 (45) (2003) 13644–13645, https://doi.org/10.1021/ja037363u.
- [15] J. Zhao, A.S. Goldman, J.F. Hartwig, Oxidative Addition of Ammonia to Form a Stable Monomeric Amido Hydride Complex, Science 307 (5712) (2005) 1080–1082. http://www.sciencemag.org/cgi/content/full/307/5712/1080.
- [16] D.Y. Wang, Y. Choliy, M.C. Haibach, J.F. Hartwig, K. Krogh-Jespersen, A. S. Goldman, Assessment of the Electronic Factors Determining the Thermodynamics of "Oxidative Addition" of C-H and N-H Bonds to Ir(I) Complexes, J. Am. Chem. Soc. 138 (1) (2016) 149–163, https://doi.org/10.1021/jacs.5b09522
- [17] J. Choi, D.Y. Wang, S. Kundu, Y. Choliy, T.J. Emge, K. Krogh-Jespersen, A. S. Goldman, Net Oxidative Addition of C(sp3)-F Bonds to Iridium via Initial C-H Bond Activation, Science 332 (2011) 1545–1548. http://www.sciencemag.org/content/332/6037/1545.
- [18] J.-I. Ito, T. Shiomi, H. Nishiyama, Efficient preparation of new rhodium- and iridium-[bis(oxazolinyl)-3,5-dimethylphenyl] complexes by C-H bond activation: applications in asymmetric synthesis, Adv. Synth. Catal. 348 (2006) 1235–1240, https://doi.org/10.1002/adsc.200606049.
- [19] J.-I. Ito, T. Kaneda, H. Nishiyama, Intermolecular C-H Bond Activation of Alkanes and Arenes by NCN Pincer Iridium(III) Acetate Complexes Containing Bis (oxazolinyl)phenyl Ligands, Organometallics 31 (2012) 4442–4449, https://doi. org/10.1021/pm3002137
- [20] C.P. Owens, A. Varela-Alvarez, V. Boyarskikh, D.G. Musaev, H.M.L. Davies, S. B. Blakey, Iridium(III)-bis(oxazolinyl)phenyl catalysts for enantioselective C-H functionalization, Chem. Sci. 4 (6) (2013) 2590–2596, https://doi.org/10.1039/C3SC50886B.
- [21] K.E. Allen, D.M. Heinekey, A.S. Goldman, K.I. Goldberg, Alkane Dehydrogenation by C-H Activation at Iridium(III), Organometallics 32 (6) (2013) 1579–1582, https://doi.org/10.1021/om301267c.
- [22] D.R. Pahls, K.E. Allen, K.I. Goldberg, T.R. Cundari, Understanding the Effect of Ancillary Ligands on Concerted Metalation-Deprotonation by (dmPhebox)Ir(OAc)2 (H2O) Complexes: A DFT Study, Organometallics 33 (22) (2014) 6413–6419, https://doi.org/10.1021/om500752m.
- [23] M. Zhou, S.I. Johnson, Y. Gao, T.J. Emge, R.J. Nielsen, W.A. Goddard, A. S. Goldman, Activation and Oxidation of Mesitylene C-H Bonds by (Phebox)Iridium (III) Complexes, Organometallics 34 (12) (2015) 2879–2888. http://pubs.acs.org/doi/abs/10.1021/acs.organomet.5b00200.
- [24] N. Li, W.-J. Zhu, J.-J. Huang, X.-Q. Hao, J.-F. Gong, M.-P. Song, Chiral NCN Pincer Iridium(III) Complexes with Bis(imidazolinyl)phenyl Ligands: Synthesis and Application in Enantioselective C-H Functionalization of Indoles with α-Aryl-α-diazoacetates, Organometallics 39 (12) (2020) 2222–2234, https://doi.org/ 10.1021/acs.organomet.0c00174.
- [25] X. Zhou, S. Malakar, T. Dugan, K. Wang, A. Sattler, D.O. Marler, T.J. Emge, K. Krogh-Jespersen, A.S. Goldman, Alkane Dehydrogenation Catalyzed by a Fluorinated Phebox Iridium Complex, ACS Catal. 11 (22) (2021) 14194–14209, https://doi.org/10.1021/acscatal.1c03562.
- [26] M. Stol, D.J.M. Snelders, M.D. Godbole, R.W.A. Havenith, D. Haddleton, G. Clarkson, M. Lutz, A.L. Spek, G.P.M. Van Klink, G. Van Koten, 2,6-Bis (oxazolinyl)phenylnickel(II) Bromide and 2,6-Bis(ketimine)phenylnickel(II) Bromide: Synthesis, Structural Features, and Redox Properties, Organometallics 26 (16) (2007) 3985–3994, https://doi.org/10.1021/om061055y.

- [27] S.H. Oakley, M.P. Coogan, R.J. Arthur, Synthesis of Bis(imino)aryl Iridium Pincer Complexes and Demonstration of Catalytic Hydrogen-Transfer Activity, Organometallics 26 (9) (2007) 2285–2290, https://doi.org/10.1021/om070059f.
- [28] G.P. Rosini, F. Liu, K. Krogh-Jespersen, A.S. Goldman, C. Li, S.P. Nolan, Thermodynamics of Addition of H2, CO, N2, and C-H Bonds to M(PiPr3)2Cl (M = Ir, Rh). An Unprecedented Metal Carbonyl Bond Strength, J. Am. Chem. Soc. 120 (36) (1998) 9256–9266, https://doi.org/10.1021/ja974100p.
- [29] K. Wang, G.P. Rosini, S.P. Nolan, A.S. Goldman, Thermodynamics of Addition of CO, Isocyanide, and H2 to Rh(PR3)2Cl, J. Am. Chem. Soc. 117 (18) (1995) 5082–5088, https://doi.org/10.1021/ja00123a010.
- [30] C.Y. Zhao, D.G. Truhlar, The M06 Suite of Density Functionals for Main Group Thermochemistry, Kinetics, Noncovalent Interactions, Excited States, and Transition Elements: Two New Functionals and Systematic Testing of Four M06 Functionals and Twelve Other Functionals, Theo. Chem. Acc. 120 (2008) 215–241, https://doi.org/10.1007/s00214-007-0310-x.
- [31] R. Ditchfield, W. J. Hehre, J. A. Pople, Self-consistent molecular-orbital methods. IX. Extended Gaussian-type basis for molecular-orbital studies of organic molecules, J. Chem. Phys. 54 (2) (1971) 724-728, https://doi.org/10.1063/ 1.1674902.
- [32] W. J. Hehre, R. Ditchfield, J. A. Pople, Self—Consistent Molecular Orbital Methods. XII. Further Extensions of Gaussian—Type Basis Sets for Use in Molecular Orbital Studies of Organic Molecules, J. Chem. Phys. 56 (5) (1972) 2257-2261, https://doi.org/10.1063/1.1677527.
- [33] P.C. Hariharan, J.A. Pople, The influence of polarization functions on molecular orbital hydrogenation energies, Theor. Chim. Acta 28 (3) (1973) 213–222, https://doi.org/10.1007/BF00533485.
- [34] P.C. Hariharan, J.A. Pople, Accuracy of AH_n equilibrium geometries by single determinant molecular orbital theory, Mol. Phys. 27 (1) (1974) 209–214, https:// doi.org/10.1080/00268977400100171.
- [35] M.M. Francl, W.J. Pietro, W.J. Hehre, J.S. Binkley, M.S. Gordon, D.J. DeFrees, J. A. Pople, Self-consistent molecular orbital methods XXIII A polarization-type basis set for second-row elements, J. Chem. Phys. 77 (7) (1982) 3654–3665, https://doi. org/10.1063/1.444267.
- [36] D. Andrae, U. Haeussermann, M. Dolg, H. Stoll, H. Preuss, Energy-adjusted ab initio pseudopotentials for the second and third row transition elements, Theor. Chim. Acta 77 (2) (1990) 123–141, https://doi.org/10.1007/BF01114537.
- [37] This root-mean-square value was not taken from the deviations between experiment and calculated values shown in Table 1, which are specifically relative to ethylene and therefore any such error determination would put undue weight on the values calculated and measure for ethylene in particular. Instead relative values were extrapolated for all L/L' couples and the root-mean-square calculation was based on those values.
- [38] The calculated global minimum for (XyPhDI)IrH₂ is a dihydrogen complex (with the H₂ ligand coordinated trans to the Ir-bound carbon, oriented in the plane of the pincer backbone). For purposes of comparison to the addition of L to (XyPhDI)IrBr₂, in which the global minimum structure has mutually trans Br ligands (both cis to the Ir-bound carbon) for (XyPhDI)IrH₂L Ir-L BDEs we calculated addition to an analogous structure of trans-(XyPhDI)IrH₂, which is actually a local energy minimum, 8.4 kcal/mol in free energy above the global minimum (XyPhDI)Ir(H₂).
- [39] M.D. Fryzuk, Side-on End-on Bound Dinitrogen: An Activated Bonding Mode That Facilitates Functionalizing Molecular Nitrogen, Acc. Chem. Res. 42 (1) (2009) 127–133, https://doi.org/10.1021/ar800061g.
- [40] Calculated (NBO) electron occupancies of the pi* orbitals of the N₂ and CO ligands of the respective complexes are calculated to be: 1-N₂, 0.102 e; 2-N₂, 0.175 e; 3-N₂, 0.269 e; 1-CO, 0.238 e; 2-CO, 0.323 e; 3-CO, 0.394 e.
- [41] R.H. Crabtree, in: The Organometallic Chemistry of the Transition Metals, 7th edn., John Wiley & Sons, Hoboken, NJ, 2019, p. 100.
- [42] J.F. Hartwig, in: Organotransition Metal Chemistry, University Science Books, Sausalito, CA, 2010, p. 36.
- [43] L. Falivene, R. Credendino, A. Poater, A. Petta, L. Serra, R. Oliva, V. Scarano, L. Cavallo, SambVca 2. A Web Tool for Analyzing Catalytic Pockets with Topographic Steric Maps, Organometallics 35 (13) (2016) 2286–2293, https://doi. org/10.1021/acs.organomet.6b00371.
- [44] L. Falivene, Z. Cao, A. Petta, L. Serra, A. Poater, R. Oliva, V. Scarano, L. Cavallo, Towards the online computer-aided design of catalytic pockets, Nat. Chem. 11 (10) (2019) 872–879, https://doi.org/10.1038/s41557-019-0319-5.
- [45] J. Rohonczy, E. Loránd, DNMR Lineshape Analysis Software Manual Version 1.1 Rev. 071103, Bruker BioSpin GmbH, TopSpin 2 (2007) 1.
- [46] D.B. Bagal, B.M. Bhanage, Recent Advances in Transition Metal-Catalyzed Hydrogenation of Nitriles, Adv. Synth. Catal. 357 (5) (2015) 883–900, https://doi. org/10.1002/adsc.201400940.
- [47] C.S. Chin, B. Lee, Hydrogenation of nitriles with iridium-triphenylphosphine complexes, Catalysis Letters 14 (1) (1992) 135–140, https://doi.org/10.1007/ PED0754229

- [48] See Supporting Information for a somewhat more detailed proposal of the full mechanism.
- [49] Y. Nakao, Metal-mediated C-CN Bond Activation in Organic Synthesis, Chem. Rev. 121 (1) (2021) 327–344, https://doi.org/10.1021/acs.chemrev.0c00301.
- [50] D. Churchill, J.H. Shin, T. Hascall, J.M. Hahn, B.M. Bridgewater, G. Parkin, The Ansa Effect in Permethylmolybdenocene Chemistry: A [Me2Si] Ansa Bridge Promotes Intermolecular C–H and C–C Bond Activation, Organometallics 18 (13) (1999) 2403–2406, https://doi.org/10.1021/om990195n.
- [51] F.L. Taw, P.S. White, R.G. Bergman, M. Brookhart, Carbon—Carbon Bond Activation of R—CN (R = Me, Ar, iPr, tBu) Using a Cationic Rh(III) Complex, J. Am. Chem. Soc. 124 (16) (2002) 4192–4193, https://doi.org/10.1021/ja0255094.
- [52] F.L. Taw, A.H. Mueller, R.G. Bergman, M. Brookhart, A Mechanistic Investigation of the Carbon-Carbon Bond Cleavage of Aryl and Alkyl Cyanides Using a Cationic Rh(III) Silyl Complex, J. Am. Chem. Soc. 125 (32) (2003) 9808–9813, https://doi. org/10.1021/ja0344680.
- [53] H. Nakazawa, T. Kawasaki, K. Miyoshi, C.H. Suresh, N. Koga, C—C Bond Cleavage of Acetonitrile by a Carbonyl Iron Complex with a Silyl Ligand, Organometallics 23 (1) (2004) 117–126, https://doi.org/10.1021/om0208319.
- [54] T. Lu, X. Zhuang, Y. Li, S. Chen, C—C Bond Cleavage of Acetonitrile by a Dinuclear Copper(II) Cryptate, J. Am. Chem. Soc. 126 (15) (2004) 4760–4761, https://doi. org/10.1021/ja031874z.
- [55] H. Nakazawa, K. Kamata, M. Itazaki, Catalytic C-C bond cleavage and C-Si bond formation in the reaction of RCN with Et3SiH promoted by an iron complex, Chem. Commun. 31 (2005) 4004–4006, https://doi.org/10.1039/B504131G.
- [56] F. Xu, W. Huang, X.-Z. You, Novel cyano-bridged mixed-valent copper complexes formed by completely in situ synthetic method via the cleavage of C-C bond in acetonitrile, Dalton Trans. 39 (44) (2010) 10652–10658, https://doi.org/10.1039/ CODT00345.I.
- [57] J.J. Garcia, A. Arevalo, N.M. Brunkan, W.D. Jones, Cleavage of Carbon-Carbon Bonds in Alkyl Cyanides Using Nickel(0), Organometallics 23 (16) (2004) 3997–4002, https://doi.org/10.1021/om049700t.
- [58] N.M. Brunkan, D.M. Brestensky, W.D. Jones, Kinetics, Thermodynamics, and Effect of BPh3 on Competitive C-C and C-H Bond Activation Reactions in the Interconversion of Allyl Cyanide by [Ni(dippe)], J. Am. Chem. Soc. 126 (11) (2004) 3627–3641, https://doi.org/10.1021/ja037002e.
- [59] T.A. Atesin, T. Li, S. Lachaize, W.W. Brennessel, J.J. Garcia, W.D. Jones, Experimental and Theoretical Examination of C-CN and C-H Bond Activations of Acetonitrile Using Zerovalent Nickel, J. Am. Chem. Soc. 129 (24) (2007) 7562–7569. https://doi.org/10.1021/ja0707153.
- [60] M.E. Evans, T. Li, W.D. Jones, C-H vs. C-C Bond activation of acetonitrile and benzonitrile via oxidative addition: rhodium vs. nickel and Cp* vs. Tp' (Tp' = hydrotris(3,5-dimethylpyrazol-1-yl)borate, Cp* = h5pentamethylcyclopentadienyl), J. Am. Chem. Soc. 132 (2010) 16278–16284, https://doi.org/10.1021/ia107927b.
- [61] T. Li, J.J. Garcia, W.W. Brennessel, W.D. Jones, C-CN Bond activation of aromatic nitriles and fluxionality of the h²-arene intermediates: experimental and theoretical investigations, Organometallics 29 (2010) 2430–2445, https://doi.org/10.1021/ om100001m
- [62] T. Tanabe, M.E. Evans, W.W. Brennessel, W.D. Jones, C-H and C-CN Bond Activation of Acetonitrile and Succinonitrile by [Tp'Rh(PR3)], Organometallics 30 (4) (2011) 834–843, https://doi.org/10.1021/om101002m.
- [63] L. Munjanja, C. Torres-López, W.W. Brennessel, W.D. Jones, C-CN Bond Cleavage Using Palladium Supported by a Dippe Ligand, Organometallics 35 (11) (2016) 2010–2013. https://doi.org/10.1021/acs.organomet.6b00304.
- [64] C.A. Tolman, W.C. Seidel, J.D. Druliner, P.J. Domaille, Catalytic hydrocyanation of olefins by nickel(0) phosphite complexes effects of Lewis acids, Organometallics 3 (1) (1984) 33–38, https://doi.org/10.1021/om00079a008.
 [65] J. Huang, C.M. Haar, S.P. Nolan, J.E. Marcone, K.G. Moloy, Lewis Acids Accelerate
- [65] J. Huang, C.M. Haar, S.P. Nolan, J.E. Marcone, K.G. Moloy, Lewis Acids Accelerate Reductive Elimination of RCN from P2Pd(R)(CN), Organometallics 18 (3) (1999) 297–299, https://doi.org/10.1021/om980897x.
- [66] J.E. Marcone, K.G. Moloy, Kinetic Study of Reductive Elimination from the Complexes (Diphosphine)Pd(R)(CN), J. Am. Chem. Soc. 120 (33) (1998) 8527–8528, https://doi.org/10.1021/ja980762i.
- [67] J. Ledford, C.S. Shultz, D.P. Gates, P.S. White, J.M. DeSimone, M. Brookhart, Bond Angle Effects on the Migratory Insertion of Ethylene and Carbon Monoxide into Palladium(II)—Methyl Bonds in Complexes Bearing Bidentate Phosphine Ligands, Organometallics 20 (25) (2001) 5266–5276, https://doi.org/10.1021/ om010489k.
- [68] T. Zhou, S. Malakar, S.L. Webb, K. Krogh-Jespersen, A.S. Goldman, Polar molecules catalyze CO insertion into metal-alkyl bonds through the displacement of an agostic C-H bond, Proc. Natl. Acad. Sci. 116 (9) (2019) 3419–3424, https://doi. org/10.1073/pnas.1816339116.